All-Optical Control of the Ultrafast Dynamics of a Hybrid Plasmonic System

Tobias Utikal,[1,2] Mark I. Stockman,[1,2,3] Albert P. Heberle,[1] Markus Lippitz,[1,2] and Harald Giessen[1]

[1]*4th Physics Institute and Research Center SCoPE, University of Stuttgart, Pfaffenwaldring 57, 70550 Stuttgart, Germany*

[2]*Max Planck Institute for Solid State Research, Heisenbergstraße 1, 70569 Stuttgart, Germany*

[3]*Department of Physics and Astronomy, Georgia State University, Atlanta, Georgia 30303, USA*

(Received 28 October 2009; revised manuscript received 17 February 2010; published 19 March 2010)

We demonstrate complete all-optical and phase-stable control of the linear optical polarization and the nonlinear coherent response (third-harmonic generation) of a hybrid nanoplasmonic-photonic system. A few tens of femtoseconds after the excitation, we turn the response on and off at any given point in time and probe its temporal evolution throughout the control process with a three-pulse nonlinear optical technique. After being switched off, the polarization and the nonlinear radiation remain off permanently. All experiments agree well with numerical simulations based on a damped harmonic oscillator model.

DOI: 10.1103/PhysRevLett.104.113903 PACS numbers: 42.70.Qs, 42.65.Ky, 73.20.Mf, 78.47.J−

Periodic plasmonic nanostructures possess unique physical properties based on enhanced nanolocalized optical fields. Their numerous applications include the generation of high harmonics with EUV frequencies [1], biosensing and detection [2,3], and nanoantennas for coupling optical radiation to molecules and semiconductors [4–6]. One of the most important challenges in nanoplasmonic systems is the dynamic ultrafast control of optical processes on a femtosecond time scale [7,8]. Plasmonic control has previously been experimentally demonstrated utilizing shaped laser pulses for excitation and two-photon photoelectron emission microscopy (PEEM) for detection, which is experimentally challenging [9–12]. Another promising method for all-optical control of the ultrafast dynamics has been reported previously in several systems, such as quantum well excitons [13,14], quantum dot excitons [15], exciton-phonon polaritons [16], and phonons in photonic crystal fibers [17].

In this work, we transfer this all-optical control concept to a plasmonic system. However, the associated wide polarizability spectra and the associated short dephasing times on the order of 10 fs [18–20] are a disadvantage for such control experiments. Especially on isolated particle plasmon polariton (PPP) modes in gold nanostructures, such experiments are very difficult to carry out, even with few-cycle optical laser pulses. To circumvent this problem, the PPP is hybridized with a slowly dephasing photonic waveguide mode in a metallic photonic crystal structure to form a waveguide-plasmon-polariton (WPP) [21]. Preceding experiments have shown that the dephasing time of these WPPs can easily exceed 50 fs [22,23], which is sufficient for the desired all-optical control scheme. Our metallic photonic crystals consist of a gold wire grating on top of a dielectric hafnium dioxide (HfO_2) slab waveguide on a quartz substrate (see Fig. 1). The incident laser light excites the PPP in the gold wire. Because of the periodic arrangement of the wires, a fraction of the electromagnetic energy is coupled into the dielectric slab waveguide, experiencing relatively low losses. By carefully designing the nanostructure, the PPP is coupled to the photonic waveguide mode and we observe a relatively narrow hybrid WPP resonance at 820 nm, which very well overlaps with the laser spectrum. This narrow spectrum implies that the polarization relaxation time of the WPP mode is much longer than that of the PPP mode. This is illustrated by the simulation shown in Fig. 2(a) (dashed line) [18]. After the excitation with an 8 fs laser pulse, which is resonant with only one WPP mode, the system undergoes a long free-induction decay whose polarization relaxation is on the order of 50 fs.

The additional simulations in Fig. 2 show the all-optical control scheme of the linear polariton polarization in an

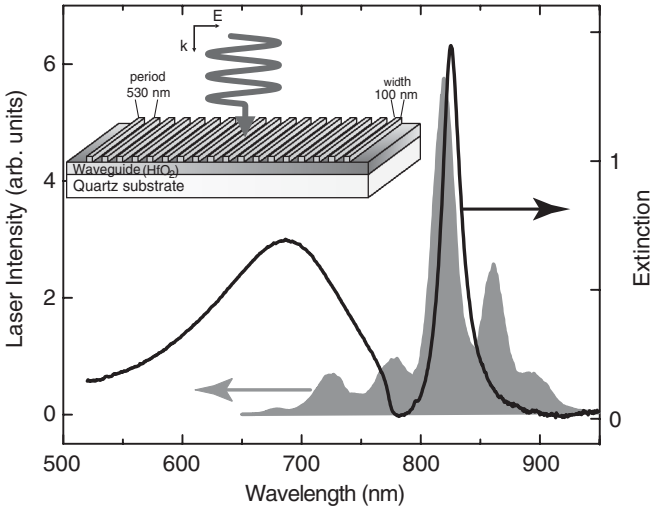

FIG. 1. Linear extinction spectrum of the nanostructure showing the two polariton modes. The laser spectrum is shown by a gray profile. Inset: Schematic of the nanostructure. Gold wires with a cross section of 100×20 nm are fabricated by electron beam lithography, spaced by a period of 530 nm atop of a 180 nm thick hafnium dioxide (HfO_2) slab waveguide on a quartz substrate.

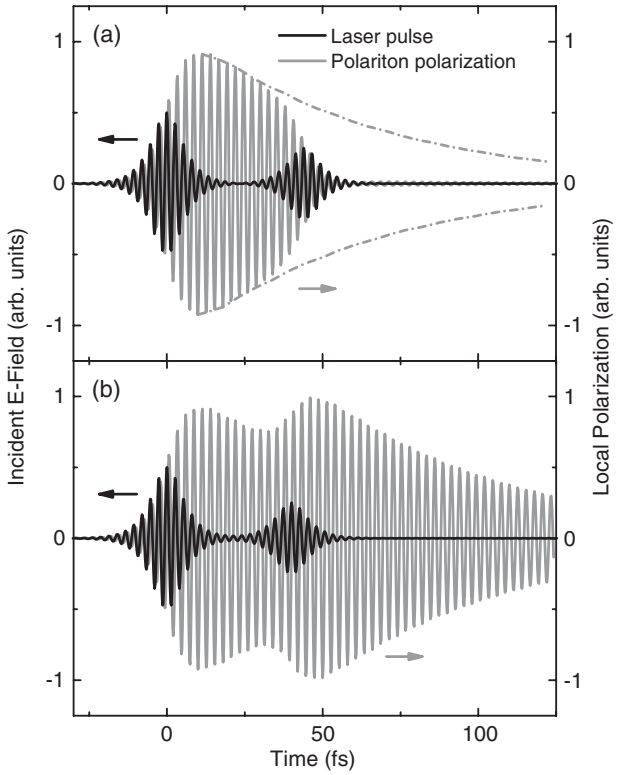

FIG. 2. Simulation of the local polariton polarization excited by a first 8 fs laser pulse and controlled by a second delayed pulse. (a) The second pulse interferes destructively with the polarization, and turns it off (destructive case). Therefore, the polarization is well below the free-induction decay (dashed line). (b) The second pulse interferes constructively with the polarization and reexcites it.

idealized system. A few tens of femtoseconds after the excitation by the first laser pulse, the second collinear pulse interferes with the slowly dephasing polarization. Dependent on the exact phase delay with respect to the first pulse, we distinguish between two extreme cases. In the first case, the second pulse interferes destructively with the polariton polarization and turns it completely off [see Fig. 2(a)]. After the second pulse, no polarization oscillations are present. In the second case, the phase delay is changed by π [a half of the oscillation period (1.33 fs)]. The second pulse now interferes constructively with the polariton polarization and enhances the oscillations [see Fig. 2(b)]. A precise choice of the amplitude of the second pulse is critical for the complete suppression in the destructive case. Because of the free-induction decay of the polarization, an oversized amplitude would lead to reexcitation and continuing oscillations of the polarization.

In this manner, the linear polariton polarization is controlled by the second laser pulse in the series. To read out the evolution of the polarization, we need a method to coherently probe the polarization during the control process at any desired time. This is done by utilizing a third laser pulse (probe pulse), whose time delay with respect to the start pulse τ_p can be tuned over a wide range. In a nonlinear optical four-photon process (third-harmonic generation, THG), the electric field of the probe pulse is mixed with the local electric field generated in the nanostructure by start and control pulse. By changing the time delay τ_p, we obtain temporally resolved information about the present polariton polarization. We note that the control is achieved by using a linear one-photon process. Because of interference with multiple pulses, the third pulse together with the nonlinear process (THG) is required to unambiguously identify the excitation and deexcitation of the polariton polarization. Note that it is this nonlinearity that makes the generated pulse integral energy be dependent on the phase of the excitation cf. Refs. [7–12].

The experimental setup is illustrated in Fig. 3(a) [24]. The first pulse (start pulse) excites the polariton polarization in the sample and defines the 0 fs position. It is followed by the second, properly attenuated control pulse, whose time delay τ_c can be set with a resolution as high as 40 as. In addition to the two pulses, we use a probe pulse, which overlaps spatially with the other pulses at the nanostructure and which is aligned at a small angle ($\phi = 3°$) with respect to start and control pulse. Because of the high pulse energies, nonlinear effects occur. Since the central symmetry of the nanostructure is not broken, second-harmonic generation is negligible; thus, third-harmonic generation is the first nonlinear order that can be detected. The oblique incidence of the probe leads to several components of the nonlinear light, which can be spatially separated behind the sample [see Fig. 3(b)]. The start and the control pulse (with the same wave vector $\mathbf{k}_1$) as well as the probe pulse (wave vector $\mathbf{k}_2$) generate the third-harmonic radiation in their respective forward directions

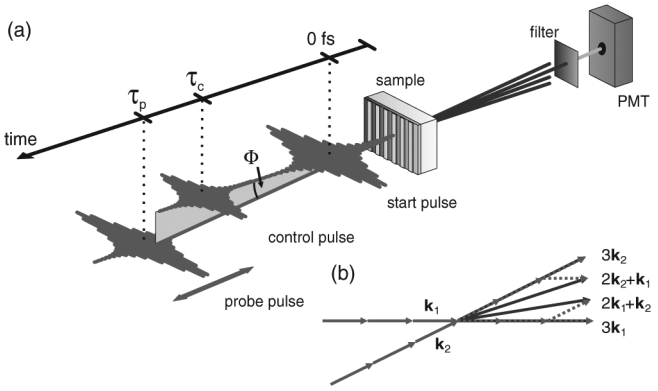

FIG. 3. (a) Schematic of the control setup. The start pulse excites the polariton polarization, and the control pulse interferes with it after the delay τ_c. The pulses are aligned with normal incidence to the sample and the electric field is polarized perpendicular to the wires. (b) In the third-harmonic regime, photons of each pulse (wave vector $\mathbf{k}_1$ and $\mathbf{k}_2$) generate higher harmonic photons in their forward directions ($3\mathbf{k}_1$ and $3\mathbf{k}_2$) and mixed photons in the directions $2\mathbf{k}_1 + \mathbf{k}_2$ and $2\mathbf{k}_2 + \mathbf{k}_1$).

(wave vectors $3\mathbf{k}_1$ and $3\mathbf{k}_2$). If the probe pulse overlaps temporally with the start or control pulse or with the fields left by them due to the polariton polarization in the system, we obtain additional background-free components in the directions $2\mathbf{k}_1 + \mathbf{k}_2$ and $2\mathbf{k}_2 + \mathbf{k}_1$ (sum THG). These sum THG signals will vanish for delays larger than τ_c if the control pulse coherently destroys the polariton polarization. They will increase in the constructive case, where the control pulse reexcites the polariton polarization. Therefore, the sum THG components deliver the necessary information about the time evolution of the polariton polarization throughout the control process. In this way, besides the linear polariton polarization, also the nonlinear optical responses in the directions $2\boldsymbol{k}_1 + \boldsymbol{k}_2$ and $2\boldsymbol{k}_2 + \boldsymbol{k}_1$ are coherently turned on and off by the control pulse on a 10 fs time scale. In the experiment, we measure therefore the third-harmonic light generated in the direction $2\mathbf{k}_2 + \mathbf{k}_1$, time integrated with a photomultiplier, as a function of the time delay τ_p between start and probe pulse.

Figures 4(a)–4(c) show the experimental results for three different time delays τ_c between start and control pulse. In a first step, we measure the nonlinear signal without the control pulse (blue curves, printed dark gray). The polarization is excited by the start pulse at 0 fs and not influenced afterwards. Therefore, the coherent free-induction decay is visible, as the oscillation amplitude decreases for larger probe pulse delays τ_p. The oscillations with a period of 2.66 fs are closely related to the polariton polarization oscillating in the nanostructure [24]. Now we turn on the control pulse (marked by the arrows) and choose the phase delay for the destructive case. The red curves (printed gray) show that the coherent nonlinear signal is again present after the start pulse but is indeed suppressed after the control pulse. No oscillations are visible for larger time delays and the signal is well below the blue curve. This clearly proves that the polariton polarization has been significantly turned off by the control pulse, and it stays off afterwards. If we shift the control pulse by another half wave period (1.33 fs), we set the phase delay for the constructive case. Now the polariton polarization is reexcited by the control pulse (green curves, printed light gray). We obtain large oscillations in the sum THG signal after the control pulse, which are well above the free-induction decay. The three data sets prove that we are able to impose the control on the system at any time within its coherence time. Additionally, the nonlinear signals are superimposed by a beating with a period of approximately 20 fs, which arises from the slight excitation of the second WPP mode at 690 nm. Since the probe pulse is not instantaneous in time and also interacts with the WPP mode, we obtain a

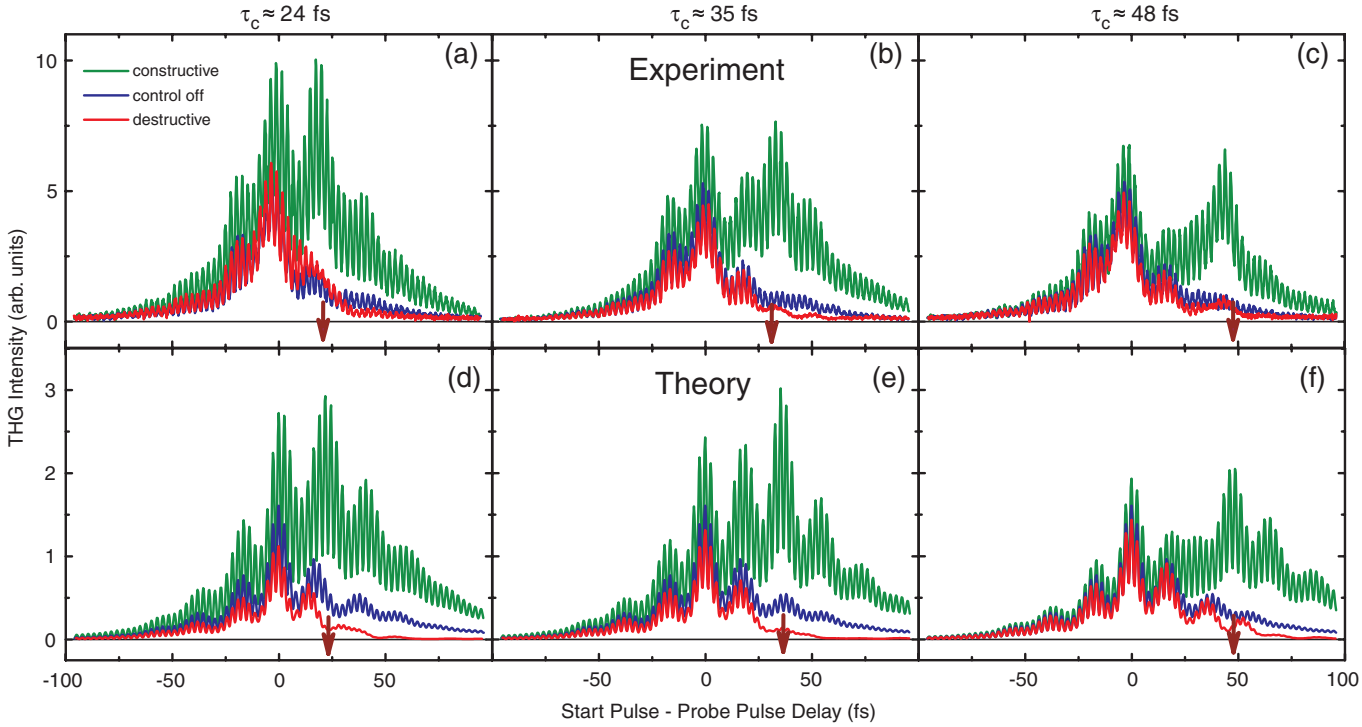

FIG. 4 (color online). (a)–(c) Experimental results of the coherent nonlinear signal in the direction $2\mathbf{k}_2 + \mathbf{k}_1$ as a function of the time delay τ_p between start and probe pulse for three different delays of the control pulse ($\tau_c \approx 24$, 35, and 48 fs, marked by the arrows). For the blue line (printed dark gray), the control pulse is switched off, and the free-induction decay of the hybrid mode is visible. The red line (printed gray) always indicates the destructive case. The polariton polarization is turned off after the control pulse and stays off. The green lines (printed light gray) show the constructive case. Here, the polariton polarization is reexcited. (d)–(f) Theoretical results for the coherent nonlinear signal corresponding to panels (a)–(c).

signal at negative time delays. Figure 4(c) shows that the contrast between the destructive case and the free-induction decay is not as high as for the smaller control pulse delays since the polariton polarization has already nearly completely dephased after 48 fs. For a control pulse delay of $\tau_c = 35$ fs [Fig. 4(b)], we measure a high contrast of about 20:1 between the constructive and the destructive case at around 67 fs after the excitation. This makes the system suitable for ultrafast plasmonic switching, with mechanisms different from Ref. [25].

We are also able to simulate the coherent nonlinear signal utilizing numerical calculations, which are based on a harmonic oscillator model [22,24]. Figures 4(d)–4(f) show the theoretical results for the three different time delays τ_c. We find an excellent agreement with the experimental data for all time delays τ_p and τ_c. In the destructive cases, the oscillations are always present after the start pulse but completely suppressed after the control pulse and stay well below the free-induction decay for all times $\tau_p > \tau_c$. In the constructive cases, we observe reinforced oscillations. Even the beating is well reproduced.

In conclusion, this work shows for the first time complete ultrafast control of a nanoplasmonic-photonic system and its nonlinear optical response on a femtosecond time scale utilizing a coherent nonlinear four-photon effect. It proves that the plasmonic polaritonic polarization and the third-harmonic radiation can be turned off completely at any time after the excitation, remaining off afterwards. The high contrast between the reexcited and the suppressed polarization makes this concept suitable for ultrafast plasmonic switching and memory.

The authors express gratitude to S. T. Cundiff, C. Lienau, M. Wegener, and T. Zentgraf for valuable comments and critiques. The discussion with the group of T. Meier is gratefully acknowledged. This work was financially supported by the German Bundesminister für Bildung und Forschung (FKZ 13N9155, 13N10146), the Deutsche Forschungsgemeinschaft (FOR 730, FOR557, and SPP1391), and the Landesstiftung Baden-Württemberg. The work of M. I. S. was supported by grants from the Chemical Sciences, Biosciences, and Geosciences Division of the Office of Basic Energy Sciences, Office of Science, U. S. Department of Energy, Grant No. CHE-0507147 from NSF, and a grant from the US-Israel BSF. A partial support of M. I. S. during his sabbatical stay at Stuttgart also came from the Max Planck Institute for Solid State Research, Stuttgart.

[1] S. Kim, J. H. Jin, Y. J. Kim, I. Y. Park, Y. Kim, and S. W. Kim, Nature (London) **453**, 757 (2008).

[2] N. Nagatani, R. Tanaka, T. Yuhi, T. Endo, K. Kerman, Y. Takamura, and E. Tamiya, Sci. Tech. Adv. Mater. **7**, 270 (2006).

[3] J. N. Anker, W. P. Hall, O. Lyandres, N. C. Shah, J. Zhao, and R. P. V. Duyne, Nature Mater. **7**, 442 (2008).

[4] P. Mühlschlegel, H. J. Eisler, O. J. F. Martin, B. Hecht, and D. W. Pohl, Science **308**, 1607 (2005).

[5] T. Kalkbrenner, U. Håkanson, A. Schädle, S. Burger, C. Henkel, and V. Sandoghdar, Phys. Rev. Lett. **95**, 200801 (2005).

[6] R. J. Moerland, T. H. Taminiau, L. Novotny, N. F. V. Hulst, and L. Kuipers, Nano Lett. **8**, 606 (2008).

[7] M. I. Stockman, S. V. Faleev, and D. J. Bergman, Phys. Rev. Lett. **88**, 067402 (2002).

[8] M. I. Stockman, D. J. Bergman, and T. Kobayashi, Phys. Rev. B **69**, 054202 (2004).

[9] A. Kubo, K. Onda, H. Petek, Z. Sun, Y. S. Jung, and H. K. Kim, Nano Lett. **5**, 1123 (2005).

[10] M. Aeschlimann, M. Bauer, D. Bayer, T. Brixner, F. J. G. de Abajo, W. Pfeiffer, M. Rohmer, C. Spindler, and F. Steeb, Nature (London) **446**, 301 (2007).

[11] M. Bauer, C. Wiemann, J. Lange, D. Bayer, M. Rohmer, and M. Aeschlimann, Appl. Phys. A **88**, 473 (2007).

[12] M. Aeschlimann, M. Bauer, D. Bayer, T. Brixner, S. Cunovic, F. Dimler, A. Fischer, W. Pfeiffer, M. Rohmer, and C. Schneider *et al.*, in *Ultrafast Phenomena XVI*, edited by P. Corkum, S. di Silvestri, K. A. Nelson, E. Riedle, and R. Schoenlein (Springer, Stresa, Italy, 2008).

[13] A. P. Heberle, J. J. Baumberg, and K. Kohler, Phys. Rev. Lett. **75**, 2598 (1995).

[14] D. S. Yee, K. J. Yee, S. C. Hohng, D. S. Kim, T. Meier, and S. W. Koch, Phys. Rev. Lett. **84**, 3474 (2000).

[15] N. H. Bonadeo, J. Erland, D. Gammon, D. Park, D. S. Katzer, and D. G. Steel, Science **282**, 1473 (1998).

[16] M. U. Wehner, M. H. Ulm, D. S. Chemla, and M. Wegener, Phys. Rev. Lett. **80**, 1992 (1998).

[17] G. S. Wiederhecker, A. Brenn, H. L. Fragnito, and P. S. J. Russell, Phys. Rev. Lett. **100**, 203903 (2008).

[18] B. Lamprecht, J. R. Krenn, A. Leitner, and F. R. Aussenegg, Appl. Phys. B **69**, 223 (1999).

[19] C. Sönnichsen, T. Franzl, T. Wilk, G. von Plessen, J. Feldmann, O. Wilson, and P. Mulvaney, Phys. Rev. Lett. **88**, 077402 (2002).

[20] C. Ropers, D. J. Park, G. Stibenz, G. Steinmeyer, J. Kim, D. S. Kim, and C. Lienau, Phys. Rev. Lett. **94**, 113901 (2005).

[21] A. Christ, S. G. Tikhodeev, N. A. Gippius, J. Kuhl, and H. Giessen, Phys. Rev. Lett. **91**, 183901 (2003).

[22] T. Zentgraf, A. Christ, J. Kuhl, and H. Giessen, Phys. Rev. Lett. **93**, 243901 (2004).

[23] T. Utikal, T. Zentgraf, J. Kuhl, and H. Giessen, Phys. Rev. B **76**, 245107 (2007).

[24] See supplementary material at http://link.aps.org/supplemental/10.1103/PhysRevLett.104.113903 for further information on the experimental setup and the numerical simulations.

[25] K. F. MacDonald, Z. L. Samson, M. I. Stockman, and N. I. Zheludev, Nat. Photon. **3**, 55 (2009).